Applied Physics Letters

Nanorod orientation control by swift heavy ion irradiation

Cite as: Appl. Phys. Lett. **120**, 171602 (2022); https://doi.org/10.1063/5.0089028
Submitted: 22 February 2022 • Accepted: 19 April 2022 • Published Online: 29 April 2022

Spyridon Korkos, Ville Jantunen, Kai Arstila, et al.

Applied Physics Letters ARTICLE scitation.org/journal/apl

Nanorod orientation control by swift heavy ion irradiation

Cite as: Appl. Phys. Lett. **120**, 171602 (2022); doi: 10.1063/5.0089028
Submitted: 22 February 2022 · Accepted: 19 April 2022 ·
Published Online: 29 April 2022

Spyridon Korkos,[1,2,a)] Ville Jantunen,[3] Kai Arstila,[1,2] Timo Sajavaara,[1,2] Aleksi Leino,[3] Kai Nordlund,[3] and Flyura Djurabekova[3]

AFFILIATIONS

[1]Accelerator Laboratory, Department of Physics, University of Jyvaskyla, P.O. Box 35, FI-40014 Jyvaskyla, Finland
[2]Nanoscience Center, Department of Physics, University of Jyvaskyla, P.O. Box 35, FI-40014 Jyvaskyla, Finland
[3]Department of Physics, University of Helsinki, P.O. Box 43, FI-00014 Helsinki, Finland

[a)]Author to whom correspondence should be addressed: spyridon.s.korkos@jyu.fi

ABSTRACT

Highly energetic ions have been previously used to modify the shape of metal nanoparticles embedded in an insulating matrix. In this work, we demonstrate that under suitable conditions, energetic ions can be used not only for shape modification but also for manipulation of nanorod orientation. This observation is made by imaging the same nanorod before and after swift heavy ion irradiation using a transmission electron microscope. Atomistic simulations reveal a complex mechanism of nanorod re-orientation by an incremental change in its shape from a rod to a spheroid and further back into a rod aligned with the beam.

Shape modification of metallic nanoparticles (NPs) has been studied for a long time as a tool for tuning the optical properties of nanocomposite materials. Spherical Au NPs have distinctive absorption peaks at visible light, which changes with size.[1] When the shape of the NPs is made cylindrical, there are two absorption peaks corresponding to transversal and longitudinal modes of surface plasmons.[1] This means that the ability to control the shapes of NPs allows for fine-tuning their response to light, making them ideal candidates for future nanoscale optical devices. Embedding the metal nanoparticles inside certain insulator materials, such as silica, allows keeping them protected from the environment and conserving whatever shape modifications have been achieved, including the orientation of the rods. While it may be difficult to access the NPs embedded inside the surrounding material with other methods, it is known that they can be modified using swift heavy ion (SHI) irradiation (i.e., using ions with energies $E \sim 1$ MeV/amu).[2–16]

Shape transformation of spherical metal NPs into nanorods aligned in the beam direction was initially reported by d'Orléans *et al.*[17] and confirmed in multiple studies later.[3,5–8,10–16] Several explanations, such as the overpressure model by d'Orléans *et al.*[17] and the ion hammering effect by Roorda *et al.*,[18] were suggested to explain the phenomenon. Although the ion hammering effect is expected to modify any size of NPs, SHI irradiation of NPs smaller than the track diameter did not cause the elongation effect.[12] On the other hand, the overpressure model was supported by molecular dynamics simulations[3] that gave atomistic insight on expansion of molten nanoparticles into a softened and underdense track in silica.

Most studies on SHI irradiated NPs have focused on spherical NPs, while other shapes have received less attention. In this study, we focus on gold nanorods inside a silica matrix and how they react to SHI irradiation. We chose a 45° angle of incidence; however, this choice is arbitrary and does not affect the observed result. We use transmission electron microscope (TEM) window grids as substrates to keep track of individual nanorods before and after irradiation. To understand the shape modification mechanism, we use a multiscale molecular dynamics simulation model based on a two-temperature approach[3,5,19–22] to gain further insight into the details of this process. Our experiments and simulations consistently show that swift heavy ion irradiation can be used to orient nanorods into the beam direction even when they remain fully inside the insulating matrix. This allows the flexible manipulation of the nanorod orientation without a risk of chemical contamination.

A 50 nm thick SiO_2 film was grown using plasma-enhanced chemical vapor deposition (PECVD) at 200 °C (Plasmalab80Plus by Oxford Instruments, SiH_4 and N_2O as precursors) on top of a TEM grid with 20 nm thick Si_3N_4 windows. Chemically synthesized Au nanorods (Sigma-Aldrich, diameter 20–45 nm and length 30–90 nm) were dispersed on top of the film by dropcasting. The nanorods were

then embedded by means of an additional 50 nm PECVD-SiO_2 film. The total layer thickness of 120 nm fulfills the requirements of TEM imaging. Time-of-flight elastic recoil detection analysis (ToF-ERDA) with a 1.7 MV Pelletron accelerator and an 11.9 MeV $^{63}Cu^{6+}$ beam[23] was used to measure the elemental composition of the deposited films at the Accelerator Laboratory of University of Jyväskylä.

The samples were irradiated by the 50 MeV $^{127}I^{9+}$ ion beam at 45° incidence in the TAMIA 5 MV tandem accelerator at Helsinki Accelerator Laboratory (University of Helsinki). Irradiation was performed to the fluence of 10^{14} ions/cm^2 at room temperature. Imaging of the irradiated samples was performed with a JEOL-JEM 1400 TEM operated at 120 kV. The direction of an electron beam was chosen perpendicular to the ion beam direction used in the irradiation experiments. All the steps of this procedure are shown in Fig. 1.

To understand the re-orientation during irradiation, we used the classical molecular dynamics code PARCAS,[24] which was used earlier for elongation simulations of spherical nanoparticles.[3,16] We generated a rectangular box of the Au fcc lattice and cut out of it a nanorod of the required size. Since the size of the experimental nanorods is too large for efficient MD simulations, we reduced the size of the nanorods to 18 nm in length and 10 nm in width, while keeping the same aspect ratio as in the experimental one. The nanorods were embedded inside the amorphous SiO_2 matrix similar to Ref. 25. In brief, the nanorod is first compressed by 2%, a cavity in silica is created with the shape and size of the original NP, and the NP is then fit inside the cavity so that it will expand to the empty space when it relaxes. The nanorods were initially aligned perpendicular to the ion beam direction.

Since the shape modification occurs only after high ion irradiation fluence, we adopted a similar approach to simulate the SHI effects in MD as described in Ref. 3. We used the instant energy deposition profiles that were pre-calculated using the two-temperature *i*-TS model.[26] We used energy depositon profiles corresponding to both 50 MeV I and 164 MeV Au. We used the latter since it gave more efficient dynamics shape modification at higher irradiation energy, and hence, it was computationally more feasible to reach high fluences with the higher energy. Moreover, the melting point of the simulated silica is much higher compared to the experimentally observed values (3500 vs 1995 K in experiments). To compensate for this difference, we scaled the profile of the deposited energy in silica with the ratio of the melting points. The Au atoms were given a constant deposited energy of 0.5 eV/atom.[3] This energy was sufficient to melt the nanorod completely. The interatomic potentials were Watanabe–Samela[27,28] for interactions in silica, embedded atom model-like for Au–Au interactions,[29,30] and Ziegler–Biersack–Littmark (ZBL)[31] for Au–O and Au–Si interactions.

The system relaxation was done for 50 ps at pressure and temperature control[32] toward zero pressure and 300 K temperature. After the system was relaxed, radial energy deposition was added perpendicular to the major axis of the initial nanorod at random locations. The ion impact was then simulated for 100 ps in NVE. Berendsen temperature control[32] at 300 K was used within the thin boundary regions perpendicular to the ion direction to dampen oscillations from pressure waves and to emulate cooling provided by the bulk material in the experimental samples.

We note that the 100 ps simulation time, which we used for computational efficiency of MD simulations, was not enough to reach full recrystallization of the nanorods after the impact. However, recrystallization is a critical step in the shape modification process as reported by Leino *et al.*,[2] because the volume of the amorphized Au NP is too large to trigger the continuous material flow into opening ion tracks in subsequent simulations. The NP must shrink to nearly original volume (and density) during the cooldown stage for sufficient thermal expansion during the subsequent impact. Although we used a similar method as by Leino *et al.*[2] and Amekura *et al.*[16] to account for recrystallization, we verified this method by running an independent 1-ns long MD simulation of relaxation of a modified NP, which showed that the modified shape of the NP did not change even after much slow cooling (see the supplementary material).

In the analysis of the samples, the same nanoparticle was imaged before and after irradiation, as shown in Fig. 2, where the subfigures (a) and (b) show the same area of the sample before and after irradiation, respectively, with identical magnification. Moreover, the image shows that most nanorods are far from the others, which excludes possible interactions between them.

Since the ion beam induced shape modification of nanoparticles is sensitive to the matrix material properties,[33] at first we performed the elemental composition analysis of the grown films using ToF-ERDA measurements. The analysis confirmed the close-to-stoichiometric elemental ratio of the as-grown silicon dioxide (2.04 ± 0.02) and the extensive presence of hydrogen (>7 at. %), which is known to be released from the SiO_2 thin film during a SHI impact.[34] The depth profiles and detailed description of the ToF-ERDA analysis can be found in the supplementary material.

The analysis of a series of TEM images (totally 19) reveals that the nanorods within the diameter and length range from 20 to 31 nm and 32 to 63 nm, respectively, have changed their orientation to align

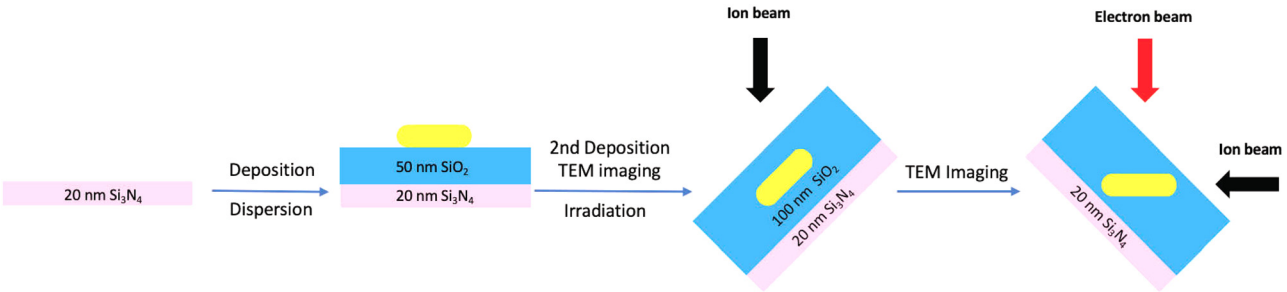

FIG. 1. Schematic representation of the experimental procedure. The sample during the second TEM stage (after irradiation) is placed in such a way that the TEM electron beam is directed perpendicular to the direction of the ion beam used during irradiation. By this way, the dimensions of the actual nanorod were imaged instead of its projection.

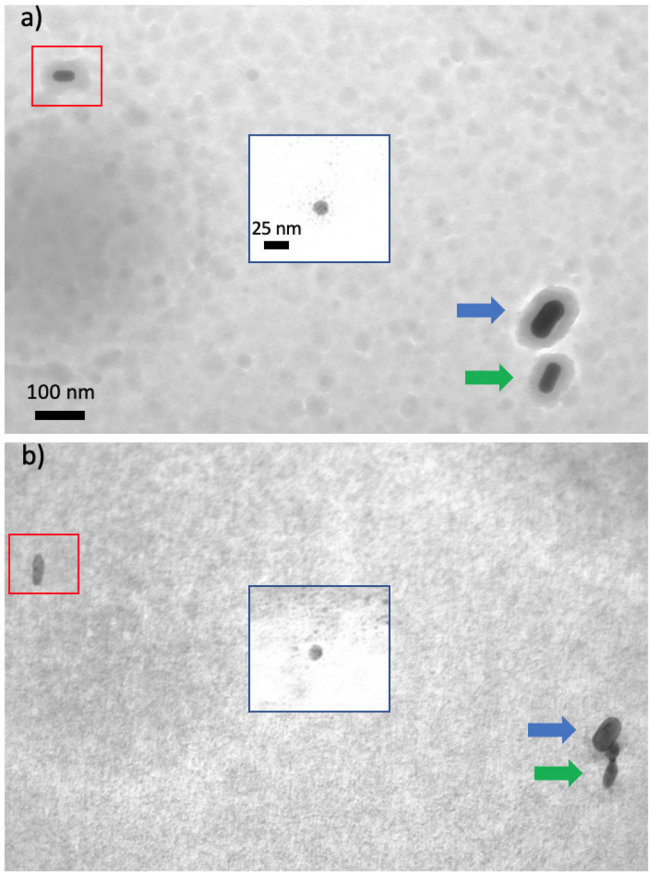

FIG. 2. TEM images of the 20 nm Si_3N_4/50 nm SiO_2/NRs/50 nm SiO_2 sample imaged (a) before and (b) after irradiation with ^{127}I at 10^{14} ions/cm^2. The images were taken (a) from the top and (b) perpendicular to the ion beam direction. (The red box outlines the nanorod, which re-orients along the ion beam direction.) The inset images in blue outline show a spherical nanoparticle (11.5 nm diameter) whose orientation did not change.

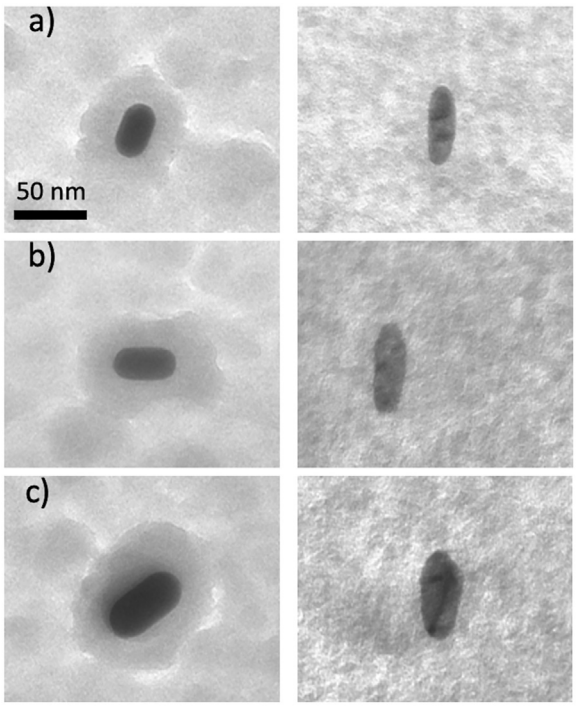

FIG. 3. TEM images of single nanorods sandwiched between two 50 nm PECVD SiO_2 layers with different initial size that re-orient along the ion beam direction after irradiation with ^{127}I at 10^{14} ions/cm^2. (a) Length = 34.3 nm and diameter = 21.2 nm, (b) length = 38.5 nm and diameter = 20.3 nm, and (c) length = 53 nm and diameter = 32 nm. (The left image is before, and the right is after irradiation.)

with the ion beam direction after the fluence of 10^{14} ions/cm^2 (see Fig. 3). This is a curious observation, since the nanorods were embedded in a homogeneous matrix, which remained intact throughout the experiment. Furthermore, the length along the major axes of the re-oriented nanorods has still visibly increased. We also note that the nanorods outside of the indicated size range have not been seen to change their orientation [compare a large nanorod indicated by a blue arrow in Figs. 2(a) and 2(b)], although the size has somewhat shrunk due to significant ion fluence. The behavior of a second large nanorod (green arrow), which is still beyond the above-mentioned range, is less clear. It is apparent that this nanorod was initially shrinking and only after its size reached the range of sizes that are seen to align with the beam, its re-orientation began. As shown in Fig. 2(b), the angle between the nanorods indicated by the blue and green arrows increased. The re-orientation, however, has not been completed, as the ion fluence received by this nanorod after its size was reduced was lower. We do not observe substantial changes in the nanorods and spherical nanoparticles that are below 15 nm in width, see the inset of Fig. 2. It is apparent that irradiation at such high ion fluences causes disintegration of the small nanoparticles and subsequent re-assembling within the track. These results are consistent with the previous work on nanospheres, which also were not found to change shape below a certain critical size.[3,13]

Furthermore, the TEM images of Fig. 3 reveal the polycrystallinity of the nanorods after irradiation. Rizza *et al.*[35] suggested that the presence of grains implies that the phase transition during the impact does not happen in the entire volume of the NP at once, but during each impact only a part of the NP melts. We, however, note here that polycrystallinity may result from fast quenching after the impact of the entirely molten NP, as shown in Ref. 3.

To understand the modification mechanism of the irradiated nanorods, we performed a series of simulations using the deposited energy profiles corresponding to 50 MeV ^{197}I and 164 MeV ^{197}Au ions. In these simulations, we saw that the first ion impacts induced formation of surface protrusions grown from the nanorods at the impact locations (see, e.g., the top left image in Fig. 4). Both deposited energy profiles gave similar results. Consecutive impacts add more localized protrusions, which gradually accumulate and cause shape transformation of the entire nanorod into at first, a spheroidal and then an elongated shape of a nanorod.

Since the dynamics of these modifications is faster under the impact of higher energy, we show in the left panel of Fig. 4 the evolution of shape modification of the nanorod irradiated by 164 MeV ^{197}Au. In comparison, similar images of the experimental nanorod are

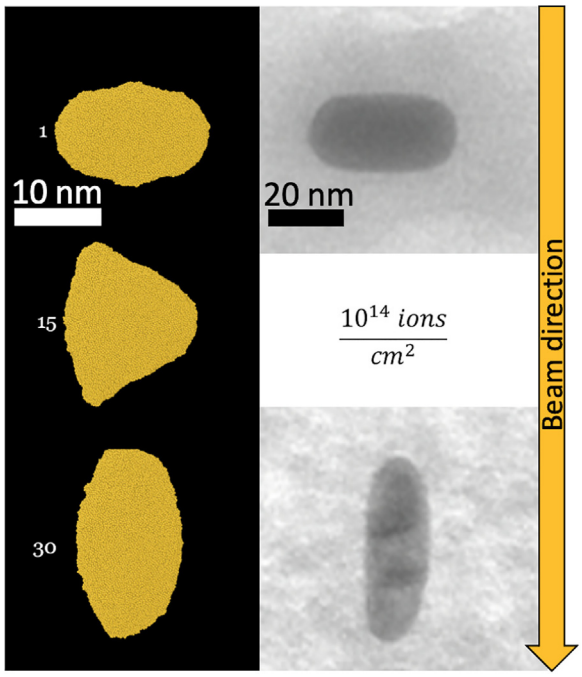

FIG. 4. Left: Nanoparticle shape after simulating 1, 15, and 30 impacts to random positions on the nanorod with 164 MeV ^{197}Au ion. Right: zoomed in of the same nanorod as in Fig. 3(b).

shown in the right panel. We follow the shape evolution by adding the ion tracks subsequently at random locations of the nanorod perpendicular to its major axis. Already after the first 15 impacts, the shape had incrementally changed to an asymmetrical spheroid, see the middle image in the left panel of Fig. 4, where the spheroid with a more elongated left side is shown. After the next 15 impacts, the shape is fully transformed into a rod in the beam direction, see the lowest image in the left panel of Fig. 4 and the corresponding experimental image on the lowest right. Although dimensions are different, the changes are proportional with similar elongation observed after irradiation in both simulation and experiment.

The simulations of ion impacts of 50 MeV ^{127}I on the same size of the nanorod are shown in Fig. 5. We see that under this energy, the shape of the nanorod changes much slower due to lower energy deposition. The results, however, are similar to those obtained for the 164 MeV ^{197}Au ions, i.e., small incremental changes transformed the nanorod oriented perpendicular to the beam into the nanorod oriented in the beam direction. Thus, we conclude that although the nanorod changes visibly its orientation, the change does not require the actual rotation within the solid matrix. The modification is guided by the dynamics of density changes in the matrix and material flow due to relaxing of the overpressured liquid phase of nanorods during the impact and fast quenching after it, as previously described for initially spherical systems.[3] The small incremental changes accumulate and result in growth in the beam direction and loss of length in others. This finally leads to a nanorod aligning in the beam direction.

We note that the irradiation conditions between the simulated and experimental nanorods are not identical. For instance, the

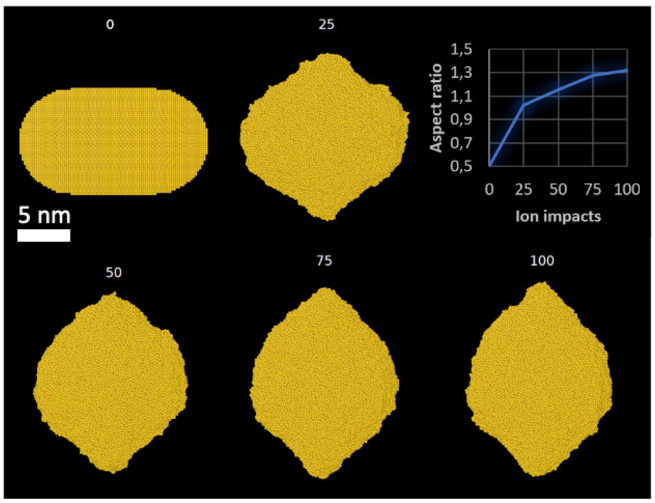

FIG. 5. Nanorod shape after 0, 25, 50, 75, and 100 simulated 50 MeV ^{127}I ion impacts to the center of the nanorod.

simulated nanorods are much smaller in size compared to those used in experiment. The numbers of ions needed to complete the re-orientation of the nanorod in simulations were 30 and 100 with the energies of 164 and 50 MeV, respectively. This corresponds to 2×10^{13} and 6.3×10^{13} ions/cm^2, i.e., the lower energy required a higher fluence to complete the re-orientation of the nanorod. The latter value of the fluence is close to the experimental fluence of 10^{14} ions/cm^2, where the ions with an energy of 50 MeV were used as well. This confirms that our MD simulations are consistent with experimental results. Moreover, a previous more detailed analysis of temperature evolution in embedded Au nanorods of different sizes due to swift heavy ion impacts further supports the presented results.[36] That work showed that the highest temperature in a nanoparticle always develops in the vicinity of ion impact, where the electron–phonon coupling is the strongest. In the nanorods of the size relevant to this study, this temperature is sufficient to cause substantial melting.

We still consider why the largest nanorods, such as the one marked with a blue arrow in Fig. 2, are not rotated. Previously, Rizza *et al.*[37] studied the size dependence of spherical nanoparticles on melting and concluded that large particles do not melt and are not deformed noticeably. In the recent study, we extended this model to nanorods including different possible interface effects on heat dynamics during the impact on a nanorod.[36] In these simulations, we saw that the energy deposited by a SHI in the large nanorods (40×80 nm^2) is not sufficient for melting even if all resistive effects for heat flow through the interface are taken into account.[36] Hence, no shape modification, including re-orientation, can be expected for very large nanorods.

In conclusion, using both experiments and simulations, we show how swift heavy ions with energies readily available in typical tandem accelerators can be used to re-orient nanorods, which are embedded in a solid amorphous matrix. In the experiments, we used TEM windows to track changes in individual nanorods. We observed that nanorods laid in a plane with a 45° angle to the beam direction re-oriented to align with the beam. By using a multiscale simulation model of the

effect of electronic excitations on atom dynamics, we explain the change in the nanorod orientation by an overpressure mechanism and show that the apparent re-orientation is a result of small incremental shape modifications rather than an actual rotation of the nanorod as a whole. Our results show that swift heavy ions even of relatively low energies can be used as a means to control the orientation of metal nanorods buried inside a protective insulating material.

See the supplementary material for the material analysis of as grown samples and the nanoparticle recrystallization in MD.

We gratefully acknowledge the Academy of Finland Novel Nanostructure Morphologies by Ion Beam Shaping (NANOIS) project (Project No. 309730) for financial support. V.J., A.L., and F.D. gratefully acknowledge IT Centre of Science CSC in Espoo, Finland for providing central processing unit resource grants.

AUTHOR DECLARATIONS

Conflict of Interest

The authors have no conflicts to disclose.

Author Contributions

S.K. conducted the experiments and V.J. conceived the simulations. All authors discussed the results. S.K and V.J. wrote the manuscript, which was discussed and edited by all authors. S.K. and V.J. contributed equally to this work.

DATA AVAILABILITY

The data that support the findings of this study are available from the corresponding author upon reasonable request.

REFERENCES

[1]S. Link and M. A. El-Sayed, "Spectral properties and relaxation dynamics of surface plasmon electronic oscillations in gold and silver nanodots and nanorods," J. Phys. Chem. B **103**, 8410–8426 (1999).
[2]A. A. Leino, O. H. Pakarinen, F. Djurabekova, and K. Nordlund, "A study on the elongation of embedded au nanoclusters in SiO_2 by swift heavy ion irradiation using md simulations," Nucl. Instrum. Methods Phys. Res., Sect. B **282**, 76–80 (2012).
[3]A. A. Leino, O. Pakarinen, F. Djurabekova, K. Nordlund, P. Kluth, and M. C. Ridgway, "Swift heavy ion shape transformation of au nanocrystals mediated by molten material flow and recrystallization," Mater. Res. Lett. **2**, 37–42 (2014).
[4]E. Dawi, A. Vredenberg, G. Rizza, and M. Toulemonde, "Ion-induced elongation of gold nanoparticles in silica by irradiation with Ag and Cu swift heavy ions: Track radius and energy loss threshold," Nanotechnology **22**, 215607 (2011).
[5]O. Peña-Rodríguez, A. Prada, J. Olivares, A. Oliver, L. Rodríguez-Fernández, H. G. Silva-Pereyra, E. Bringa, J. M. Perlado, and A. Rivera, "Understanding the ion-induced elongation of silver nanoparticles embedded in silica," Sci. Rep. **7**, 922 (2017).
[6]C. d'Orleans, J. Stoquert, C. Estournes, J. Grob, D. Muller, J. Guille, M. Richard-Plouet, C. Cerruti, and F. Haas, "Elongated co nanoparticles induced by swift heavy ion irradiations," Nucl. Instrum. Methods Phys. Res., Sect. B **216**, 372–378 (2004).
[7]S. Klaumünzer, "Modification of nanostructures by high-energy ion beams," Nucl. Instrum. Methods Phys. Res., Sect. B **244**, 1–7 (2006).
[8]K. Awazu, X. Wang, M. Fujimaki, J. Tominaga, H. Aiba, Y. Ohki, and T. Komatsubara, "Elongation of gold nanoparticles in silica glass by irradiation with swift heavy ions," Phys. Rev. B **78**, 054102 (2008).
[9]K. Awazu, X. Wang, T. Komatsubara, J. Watanabe, Y. Matsumoto, S. Warisawa, and S. Ishihara, "The fabrication of aligned pairs of gold nanorods in SiO_2 films by ion irradiation," Nanotechnology **20**, 325303 (2009).
[10]E. Dawi, G. Rizza, M. Mink, A. Vredenberg, and F. Habraken, "Ion beam shaping of au nanoparticles in silica: Particle size and concentration dependence," J. Appl. Phys. **105**, 074305 (2009).
[11]P. Kluth, R. Giulian, D. Sprouster, C. Schnohr, A. Byrne, D. Cookson, and M. Ridgway, "Energy dependent saturation width of swift heavy ion shaped embedded au nanoparticles," Appl. Phys. Lett. **94**, 113107 (2009).
[12]D. Avasthi, Y. Mishra, F. Singh, and J. Stoquert, "Ion tracks in silica for engineering the embedded nanoparticles," Nucl. Instrum. Methods Phys. Res., Sect. B **268**, 3027–3034 (2010).
[13]M. C. Ridgway, R. Giulian, D. J. Sprouster, P. Kluth, L. L. Araújo, D. Llewellyn, A. Byrne, F. Kremer, P. F. P. Fichtner, G. Rizza *et al.*, "Role of thermodynamics in the shape transformation of embedded metal nanoparticles induced by swift heavy-ion irradiation," Phys. Rev. Lett. **106**, 095505 (2011).
[14]H. Amekura, N. Ishikawa, N. Okubo, M. C. Ridgway, R. Giulian, K. Mitsuishi, Y. Nakayama, C. Buchal, S. Mantl, and N. Kishimoto, "Zn nanoparticles irradiated with swift heavy ions at low fluences: Optically-detected shape elongation induced by nonoverlapping ion tracks," Phys. Rev. B **83**, 205401 (2011).
[15]Y. Mishra, F. Singh, D. Avasthi, J. Pivin, D. Malinovska, and E. Pippel, "Synthesis of elongated au nanoparticles in silica matrix by ion irradiation," Appl. Phys. Lett. **91**, 063103 (2007).
[16]H. Amekura, P. Kluth, P. Mota-Santiago, I. Sahlberg, V. Jantunen, A. A. Leino, H. Vázquez, K. Nordlund, F. Djurabekova, N. Okubo *et al.*, "Vaporlike phase of amorphous SiO_2 is not a prerequisite for the core/shell ion tracks or ion shaping," Phys. Rev. Mater. **2**, 096001 (2018).
[17]C. d'Orléans, J. Stoquert, C. Estournes, C. Cerruti, J. Grob, J. Guille, F. Haas, D. Muller, and M. Richard-Plouet, "Anisotropy of Co nanoparticles induced by swift heavy ions," Phys. Rev. B **67**, 220101 (2003).
[18]S. Roorda, T. van Dillen, A. Polman, C. Graf, A. van Blaaderen, and B. J. Kooi, "Aligned gold nanorods in silica made by ion irradiation of core–shell colloidal particles," Adv. Mater. **16**, 235–237 (2004).
[19]M. Toulemonde, W. Assmann, C. Dufour, A. Meftah, F. Studer, and C. Trautmann, "Experimental phenomena and thermal spike model description of ion tracks in amorphisable inorganic insulators," Mat. Fys. Med. **52**, 263–292 (2006).
[20]I. Lifshits, M. Kaganov, and L. Tanatarov, "On the theory of radiation-induced changes in metals," J. Nucl. Energy, Part A **12**, 69–78 (1960).
[21]S. Anisimov, B. Kapeliovich, T. Perelman *et al.*, "Electron emission from metal surfaces exposed to ultrashort laser pulses," Zh. Eksp. Teor. Fiz. **66**, 375–377 (1974).
[22]A. Leino, S. Daraszewicz, O. H. Pakarinen, K. Nordlund, and F. Djurabekova, "Atomistic two-temperature modelling of ion track formation in silicon dioxide," Europhys. Lett. **110**, 16004 (2015).
[23]M. Laitinen, M. Rossi, J. Julin, and T. Sajavaara, "Time-of-flight—Energy spectrometer for elemental depth profiling—Jyväskylä design," Nucl. Instrum. Methods Phys. Res., Sect. B **337**, 55–61 (2014).
[24]PARCAS Computer code 1996–2021, available open source at https://gitlab.com/acclab/parcas/. The main principles of the molecular dynamics algorithms are presented by Nordlund *et al.* [K. Nordlund, M. Ghaly, R. Averback, M. Caturla, T. D. de La Rubia, and J. Tarus, "Defect production in collision cascades in elemental semiconductors and fcc metals," Phys. Rev. B **57**, 7556 (1998)] and Ghaly *et al.* [M. Ghaly, K. Nordlund, and R. S. Averback, "Molecular dynamics investigations of surface damage produced by kiloelectronvolt self-bombardment of solids," Philos. Mag. A **79**, 795–820 (1999)]. The adaptive time step and electronic stopping algorithms are the same as work by K. Nordlund ["Molecular dynamics simulation of ion ranges in the 1–100 keV energy range," Comput. Mater. Sci. **3**, 448–456 (1995)]. The 2016 version of the code is published in the supplementary material to F. Granberg, K. Nordlund, M. W. Ullah, K. Jin, C. Lu, H. Bei, L. Wang, F. Djurabekova, W. Weber, and Y. Zhang, "Mechanism of radiation damage reduction in equiatomic multicomponent single phase alloys," Phys. Rev. Lett. **116**, 135504 (2016).
[25]F. Djurabekova and K. Nordlund, "Atomistic simulation of the interface structure of Si nanocrystals embedded in amorphous silica," Phys. Rev. B **77**, 115325 (2008).

[26]M. Toulemonde, W. Assmann, C. Dufour, A. Meftah, F. Studer, and C. Trautmann, "Experimental phenomena and thermal spike model description of ion tracks in amorphisable inorganic insulators," Mat. Fys. Medd. **52**, 263–292 (2006).
[27]T. Watanabe, D. Yamasaki, K. Tatsumura, and I. Ohdomari, "Improved interatomic potential for stressed si, o mixed systems," Appl. Surf. Sci. **234**, 207–213 (2004).
[28]J. Samela, K. Nordlund, V. N. Popok, and E. E. Campbell, "Origin of complex impact craters on native oxide coated silicon surfaces," Phys. Rev. B **77**, 075309 (2008).
[29]S. Foiles, M. Baskes, and M. S. Daw, "Embedded-atom-method functions for the fcc metals Cu, Ag, Au, Ni, Pd, Pt, and their alloys," Phys. Rev. B **33**, 7983 (1986).
[30]S. Foiles, M. Baskes, and M. Daw, "Erratum: Embedded-atom-method functions for the fcc metals Cu, Ag, Au, Ni, Pd, Pt, and their alloys," Phys. Rev. B **37**, 10378 (1988).
[31]J. F. Ziegler and J. P. Biersack, "The stopping and range of ions in matter," in *Treatise on Heavy-Ion Science* (Springer, 1985), pp. 93–129.
[32]H. J. Berendsen, J. v. Postma, W. F. van Gunsteren, A. DiNola, and J. R. Haak, "Molecular dynamics with coupling to an external bath," J. Chem. Phys. **81**, 3684–3690 (1984).
[33]P. Mota-Santiago, F. Kremer, A. Nadzri, M. C. Ridgway, and P. Kluth, "Elongation of metallic nanoparticles at the interface of silicon dioxide and silicon nitride," Nucl. Instrum. Methods Phys. Res., Sect. B **409**, 328–332 (2017).
[34]F. Corni, A. Monelli, G. Ottaviani, R. Tonini, G. Queirolo, and L. Zanotti, "Radiation enhanced transport of hydrogen in SiO_2," J. Non-Cryst. Solids **216**, 71–76 (1997).
[35]G. Rizza, E. Dawi, A. Vredenberg, and I. Monnet, "Ion engineering of embedded nanostructures: From spherical to facetted nanoparticles," Appl. Phys. Lett. **95**, 043105 (2009).
[36]V. E. Jantunen, A. A. Leino, M. Veske, A. Kyritsakis, H. V. Muiños, K. Nordlund, and F. Djurabekova, "Interface effects on heat dynamics in embedded metal nanoparticles during swift heavy ion irradiation," J. Phys. D: Appl. Phys. **55**, 275301 (2022).
[37]G. Rizza, P. Coulon, V. Khomenkov, C. Dufour, I. Monnet, M. Toulemonde, S. Perruchas, T. Gacoin, D. Mailly, X. Lafosse *et al.*, "Rational description of the ion-beam shaping mechanism," Phys. Rev. B **86**, 035450 (2012).